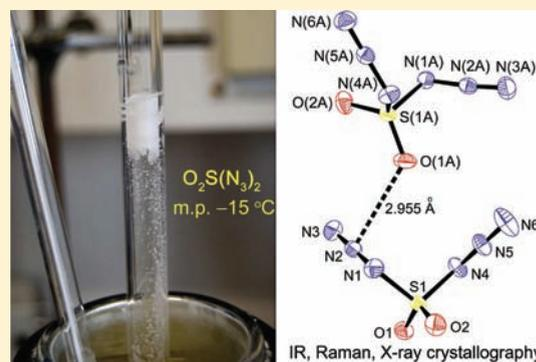


Synthesis and Characterization of Sulfuryl Diazide, $O_2S(N_3)_2$ Xiaoqing Zeng,^{*,†} Helmut Beckers,[†] Eduard Bernhardt,[†] and Helge Willner[†][†]Bergische Universität Wuppertal, FB C – Anorganische Chemie, Gauss Strasse 20, D-42097 Wuppertal, Germany

S Supporting Information

ABSTRACT: Sulfuryl diazide, $O_2S(N_3)_2$, previously described as an “exceedingly explosive” compound, has been isolated and characterized by IR (Ar matrix, gas) and Raman (solid) spectroscopy, and its structure has been determined by X-ray crystallography. It has a melting point of $-15\text{ }^\circ\text{C}$ and can be handled in small quantities in gas, liquid, and solid states. Vibrational spectroscopic studies suggest the presence of only one conformer in both gas and solid states, and the X-ray crystallography revealed an anti conformation of the two azido groups with respect to the NSN plane. Calculations predict the anti (C_2) conformer to be 6.6 kJ mol^{-1} lower in energy than the syn (C_s) one at the CBS-QB3 level of theory. The related chlorosulfuryl azide, $ClSO_2N_3$, has also been prepared and characterized by IR and Raman spectroscopy.



INTRODUCTION

Covalent azides have been widely used in organic synthesis.¹ Because of their high energy content, azides have also been well-known as high-energy materials. Because some of them are extremely heat and shock sensitive, the preparation and characterization requires sophisticated skills with appropriate safety precautions. Many novel covalent azides, particularly the polyazides of the heavy elements of group 15 (P, As, Sb, Bi)² and 16 (Se, Te)³ have recently been isolated and characterized. The azides of the light element N have been extensively explored by quantum chemical calculations, and the experimental access to these metastable species was found to be rather challenging but quite successful in very recent few years.⁴

Many organic sulfur azides have already been known and applied in synthetic chemistry, but only a few of inorganic sulfur azides have been fully characterized, such as the monoazides FSO_2N_3 ⁵ and the anions $SO_2N_3^-$, $(SO_2)_2N_3^-$, and $SO_3N_3^-$.⁶ Our knowledge about the diazides, such as $S(N_3)_2$, $OS(N_3)_2$, and $O_2S(N_3)_2$ is relatively scarce. The first one has been merely theoretically predicted,⁷ $OS(N_3)_2$ has been only detected in the gas phase by photoelectron spectroscopy.⁸ The title compound, $O_2S(N_3)_2$, has been known for nearly 100 years,⁹ and its chemistry in the solution has been reported in a few early publications.¹⁰ As has been mentioned in these studies, this azide has exceedingly explosive, unpredictable properties. In some cases, violent explosions occurred without any provocation. Therefore, no isolation or characterization of this compound was performed in previous work.

Stimulated by the recent successful isolation of the “extremely explosive” $OC(N_3)_2$ in a pure form,¹¹ we performed reactions between SO_2Cl_2 and NaN_3 , which enabled us to isolate pure $ClSO_2N_3$ and $O_2S(N_3)_2$. Herein, we describe their preparation as pure substances, their physical and spectroscopic properties as well as the structure of the diazide for the first time.

EXPERIMENTAL SECTION

Caution! Covalent azides are potentially hazardous and explosive! Sulfuryl azides, $ClSO_2N_3$, and $O_2S(N_3)_2$ are explosive compounds and should be handled in submillimolar quantities only. Safety precautions (face shields, leather gloves, and protective leather clothing) are strongly recommended, particularly in the case of handling pure $O_2S(N_3)_2$ in the solid and liquid states. The scratch and break of ampules containing shock-sensitive compounds using the ampule key technique can lead to explosion. In one case, explosion of the solid sample was experienced when the sample (ca. 20 mg) was cooled in a glass tube under liquid nitrogen, which may be caused by a solid-phase transformation.

Materials and Apparatus. Sulfuryl chloride (SO_2Cl_2 , Merck) was distilled before use, and its purity was checked by gas-phase IR spectroscopy. Sodium azide (NaN_3 , Merck) was dried at $100\text{ }^\circ\text{C}$ under vacuum before use. For the preparation of ^{15}N -labeled samples, $1\text{-}^{15}\text{N}$ sodium azide (98 atom % ^{15}N , EURISO-TOP GmbH) was used as received. Acetonitrile (CH_3CN , Merck) was dried with P_4O_{10} and distilled immediately before use. Volatile materials were manipulated in a glass vacuum line equipped with a capacitance pressure gauge (221 AHS-1000, MKS Baratron, Burlington, MA), three U-traps, and valves with PTFE stems (Young, London, UK). The vacuum line was connected to an IR gas cell (optical path length 20 cm, Si windows, 0.6 mm thick), which was fitted into the sample compartment of the FTIR instrument (Bruker, Vector 22) for measuring the IR spectra of volatile products. The final products were stored in flame-sealed glass ampules in liquid nitrogen. Glass ampules were opened to the vacuum line using an ampule key,¹² and appropriate amounts were taken out, followed by flame-sealing the ampule with the remaining sample.

Synthesis. The reactions were performed in a glass container (volume 25 mL, length 20 cm) equipped with a small magnetic stir bar and a valve with PTFE stem and connected to the vacuum line. For the preparation of sulfuryl diazide, the vessel was charged with 1.7 mmol

Received: June 16, 2011

Published: August 04, 2011

NaN₃, then 0.4 mmol SO₂Cl₂ and 1 mL CH₃CN were condensed onto the solid. The mixture was warmed to room temperature and stirred overnight. Then the vessel was slowly opened to the vacuum line and all of the volatile products were separated by repeated fractional condensation (−30, −100, and −196 °C). The desired product (ca. 50 mg), O₂S(N₃)₂, was retained in the −30 °C trap as a white solid. Traces of noncondensable gas at −196 °C were observed, indicating some decomposition of O₂S(N₃)₂ during the synthesis. When the reaction was performed without any solvent, no O₂S(N₃)₂ but only ClSO₂N₃ was isolated, which was purified by repeated fractional condensation (−30, −78, and −196 °C), and the azide was retained in the middle trap as colorless liquid. 1-¹⁵N sodium azide was used for the ¹⁵N-labeled sample in a similar manner. The quality of the samples was ascertained by gas-phase IR spectroscopy.

Spectroscopy. Raman spectra were recorded on a Bruker-Equinox 55 FRA 106/S FT-Raman spectrometer using a 1064 nm Nd:YAG laser (200 mW) with 200 scans at a resolution of 2 cm^{−1}. For the low-temperature measurement, a small amount of sample (ca. 10 mg) was condensed in a high vacuum onto a copper finger, which was cooled with liquid nitrogen. Subsequently, the coldfinger was rotated to allow the sample exposure to the laser beam.

Matrix IR spectra were recorded on a FTIR spectrometer (IFS 66v/S Bruker) in reflectance mode using a transfer optic. A KBr beam splitter and an MCT detector were used in the region of 4000 to 550 cm^{−1}. For each spectrum, 200 scans at a resolution of 0.25 cm^{−1} were co-added. The gaseous sample was mixed with argon (1:1000) in a 1 L stainless-steel storage container and then small amount (ca. 1 mmol) of the mixture was deposited within 30 min onto the cold matrix support (16 K, Rh plated Cu block) in a high vacuum. Details of the matrix apparatus have been described elsewhere.¹³

The UV–vis spectra of gas samples (1.5 mbar, room temperature) were recorded in a quartz cell (10 cm optical path length) on a PerkinElmer Lambda EZ210 spectrophotometer.

Single Crystal Structure Determination

(a). Crystal Growth and Transfer. Crystals of O₂S(N₃)₂ were grown in an L-shaped glass tube (o.d. 0.6 cm, length 20 cm). Small amounts (ca. 5 mg) of the compound were flame-sealed into one end of the bent tube, the end without sample was immersed into a cold bath at ca. −60 °C, whereas the whole setup with cold bath was kept in a refrigerator at −20 °C overnight. Small colorless crystals were obtained in the bottom of the tube in the cold bath. Because of the possible shock sensitivity, the cut of the tube and transfer of the crystals needs to be done with care, that is, the glass tube containing crystals was kept cold in a dry ice bath (ca. −78 °C) and connected to the vacuum line through an ampule key. Then the tube was opened to the vacuum and slowly filled with argon gas to one atmosphere, followed by a quick transfer of the crystals into a trough precooled by a flow of cold nitrogen. A suitable crystal of O₂S(N₃)₂ was selected at ca. −50 °C under the microscope and mounted as previously described.¹⁴

(b). Collection and Reduction of X-ray Diffraction Data.

Crystals were mounted on an Oxford Diffraction Gemini E Ultra diffractometer, equipped with a 2K × 2K EOS CCD area detector, a four-circle kappa goniometer, an Oxford Instruments Cryojet, and sealed-tube Enhanced (Mo) and an Enhanced Ultra (Cu) sources. For the data collection, the Cu source emitting monochromated Cu–Kα radiation (λ = 1.54184 Å) was used. The diffractometer was controlled by the *CrysAlis^{Pro} Graphical User Interface (GUI)* software.¹⁵ Diffraction data collection strategy for O₂S(N₃)₂ was optimized with respect to complete coverage and consisted of 10 ω scans with a width of 1°, respectively. The data collection for O₂S(N₃)₂ was carried out at −123 °C, in a 1024 × 1024 pixel mode using 2 × 2 pixel binning. Processing of the raw data, scaling of diffraction data, and the application of an empirical absorption correction was completed by using the *CrysAlis^{Pro}* program.¹⁵

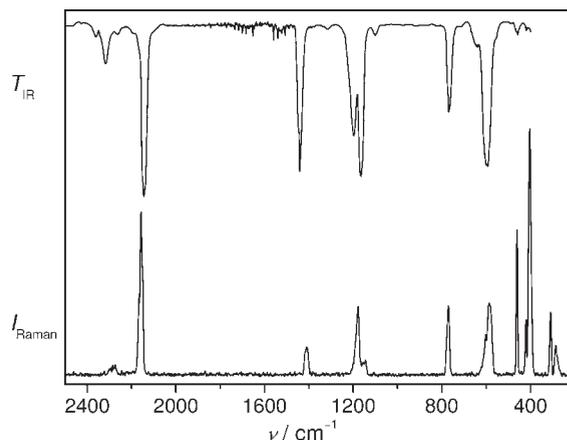


Figure 1. Upper trace: IR spectrum of gaseous ClSO₂N₃ at 298 K (transmission T_{IR} , resolution: 2 cm^{−1}). Lower trace: Raman spectrum of solid ClSO₂N₃ at 77 K (Raman intensity I_{Raman} , resolution: 2 cm^{−1}).

Table 1. Experimental and Calculated Vibrational Frequencies (cm^{−1}) of ClSO₂N₃

experimental ^a		calculated ^b	approximately description
IR	Raman		
vapor (298 K)	solid (77 K)		
2144 vs	2157 s	2273 (412)	$\nu_{\text{as}}(\text{N}_3)$
1441 s	1411 m	1442 (176)	$\nu_{\text{as}}(\text{SO}_2)$
1197 s	1178 m	1245 (254)	$\nu_{\text{s}}(\text{N}_3)$
1165 s	1145 w, sh	1199 (180)	$\nu_{\text{s}}(\text{SO}_2)$
768 m	771 m	747 (73)	$\nu(\text{SN})$
597 vs	601 w, sh	604 (184)	$\delta(\text{N}_3)$
		579 (15)	$\delta_{\text{o.o.p.}}(\text{SN}_3)$
		570 (168)	$\delta(\text{SO}_2)$
458 w	461 m	449 (4)	$\omega(\text{SO}_2)$
419 vw	421 w	413 (2)	$\rho(\text{SO}_2)$
	404 vs	371 (8)	$\nu(\text{SCl})$
	309 m	290 (<1)	$\delta(\text{OSCl})$
	285 m	267 (1)	$\delta(\text{NSCl})$
		149 (<1)	τ
		55 (<1)	τ

^a Experimental band positions and relative intensities: vs, very strong; s, strong; m, medium strong; w, weak; vw, very weak; and sh, shoulder.

^b B3LYP/6-311+G(3df) level of theory; IR intensities (km mol^{−1}) in parentheses.

(c). Solution and Refinement of the Structure. The solution of the structure was obtained by direct methods which located the positions of all atoms. The final refinement was obtained by introducing anisotropic thermal parameters and the recommended weightings for all atoms. All calculations were performed using the *SHELXTL-plus* package program for the structure determination and solution refinement and for the molecular graphics.¹⁶

Computational Details. Structures were optimized using DFT methods (B3LYP,¹⁷ BP86,¹⁸ MPW1PW91¹⁹) and the 6-311+G(3df) basis set throughout. Local minima were confirmed by harmonic frequency analyses. The complete basis set (CBS-QB3) method was used for accurate relative energies.²⁰ Natural bond orbital (NBO) analysis²¹ was performed using the B3LYP/6-311+G(3df) method for

the evaluation of donor–acceptor (lone pair–antibonding) interaction energies $E(2)$, based on second-order perturbation theory. All calculations were performed using the *Gaussian 03* software package.²²

RESULTS AND DISCUSSION

Physical Properties of $O_2S(N_3)_2$. According to previous studies,¹⁰ sulfonyl diazide can be safely handled in organic solvents,

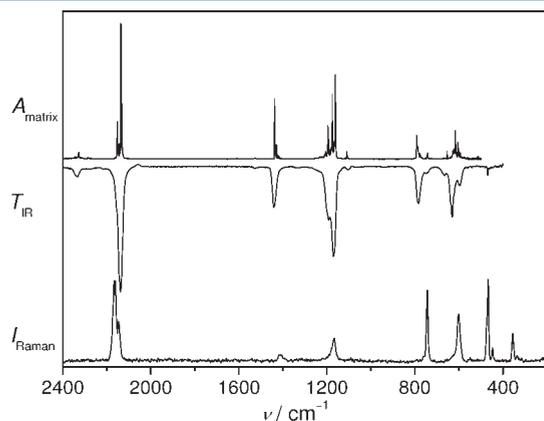


Figure 2. Upper trace: IR spectrum of $O_2S(N_3)_2$ isolated in an Ar-matrix at 16 K (absorbance A , resolution: 0.25 cm^{-1}). Middle trace: IR spectrum of gaseous $O_2S(N_3)_2$ at 298 K (transmission T , resolution: 2 cm^{-1}). Lower trace: Raman spectrum of solid $O_2S(N_3)_2$ at 77 K (Raman intensity I , resolution: 2 cm^{-1}).

but nothing has been reported for the neat compound. The compound was only handled in a small scale ($<0.1\text{ g}$, *Caution* section). The solid melts at $-15\text{ }^\circ\text{C}$ and forms a colorless liquid. The liquid has a vapor pressure of about 2 mbar at room temperature, which allows its transfer in a vacuum line. The liquid was stored in flame-sealed glass ampules at room temperature without any noticeable decomposition after a few weeks.

The UV–vis spectrum of gaseous $O_2S(N_3)_2$ resembles that of $ClSO_2N_3$ (Figure S1 of the Supporting Information). It reveals two broad absorptions at $\lambda_{\text{max}} = 260$ and 210 nm , and they are assigned to $n \rightarrow \pi^*$ and $\pi \rightarrow \pi^*$ transitions corresponding to the azido groups, respectively.

IR and Raman Spectra of $ClSO_2N_3$. To distinguish the vibrational spectra of $O_2S(N_3)_2$ from that of the monoazide $ClSO_2N_3$, the IR (gas), and Raman (solid) spectra of $ClSO_2N_3$ were measured and shown in Figure 1. Observed band positions are listed in Table 1 and compared to calculated ones at the B3LYP/6-311+G(3df) level of theory. Bands due to the SO_2 and N_3 groups are easily assigned by comparison to those of the related compound FSO_2N_3 .⁵

The IR bands of $ClSO_2N_3$ in the gas phase (2144, 1441, 1197, and 1165 cm^{-1}) agree well with those reported in CH_3CN solution (2115, 1430, 1190, and 1150 cm^{-1}).^{10b} The S–Cl stretch appears at 404 cm^{-1} in the Raman spectrum, the expected ^{35/37}Cl isotopic splitting of $\nu(SCl)$ in the intensity ratio of 3:1 was not observed. The S–N stretch (IR: 768 cm^{-1} , Raman: 771 cm^{-1}) is strongly mixed with the deformations of the N_3 and SO_2 moieties. Similar to other sulfonyl azides, only one conformer with C_1 symmetry was

Table 2. Experimental and Calculated Vibrational Frequencies (cm^{-1}) of $O_2S(N_3)_2$

experimental ^a		calculated ^b		approximately description	
IR	Raman	anti (C_2)	syn (C_s)		
vapor (298 K)	Ar-matrix (16 K) ^c	solid (77 K)			
2155 sh	2151.0 m	2163 vs	2280 (167)	2280 (457)	$\nu_{\text{as}}(N_3)$, in-phase
2137 vs	2135.1 vs	2147 s	2263 (822)	2251 (426)	$\nu_{\text{as}}(N_3)$, out-of-phase
1441 s	1437.7 s	1413 w	1446 (187)	1446 (203)	$\nu_{\text{as}}(SO_2)$
1193 m, sh	1195.9 m		1260 (101)	1275 (212)	$\nu_s(N_3)$, in-phase
1170 s	1176.9 s		1245 (450)	1250 (258)	$\nu_s(N_3)$, out-of-phase
	1161.7 s	1170 m	1201 (219)	1193 (191)	$\nu_s(SO_2)$
783 s	791.2 s		763 (133)	742 (19)	$\nu_{\text{as}}(NSN)$
748 w	744.1 w	744 s	726 (19)	741 (174)	$\nu_s(NSN)$
630 s	616.6 s	629 w, sh	626 (331)	622 (271)	$\delta(N_3)$
595 m	601.1 w	602 s	598 (88)	597 (93)	$\delta(N_3) + \delta(SO_2)$
			583 (12)	579 (13)	$\delta_{\text{o.o.p.}}(SN_3)$, in-phase
			580 (1)	571 (<1)	$\delta_{\text{o.o.p.}}(SN_3)$, out-of-phase
469 vw		467 s	456 (4)	456 (<1)	$\delta(SO_2)$
		446 w	454 (1)	455 (3)	$\omega(SO_2)$
			443 (2)	445 (3)	$\rho(SO_2)$
		355 w	341 (<1)	339 (<1)	$\tau(N_2SO_2)$
		330 vw	319 (<1)	303 (1)	$\delta(NSN)$
			160 (<1)	169 (<1)	τ
			150 (1)	150 (1)	τ
			71 (<1)	47 (<1)	τ
			39 (<1)	21 (<1)	τ

^a Experimental band positions and intensities: vs, very strong; s, strong; m, medium strong; w, weak; vw, very weak; and sh, shoulder. ^b B3LYP/6-311+G(3df) level of theory (molecular symmetry indicated in parentheses); IR intensities (km mol^{-1}) are given in parentheses. ^c Only the band positions of the most intense matrix sites are given.

Table 3. Summary of Crystal Data and Refinement Results for $O_2S(N_3)_2$

chemical formula	N_6O_2S
space group	monoclinic ($C2/c$, No. 15)
a (Å)	24.3405(7)
b (Å)	5.41599(10)
c (Å)	17.2915(4)
α (deg)	90
β (deg)	111.819(3)
γ (deg)	90
V (Å ³)	2116.21(9)
Z (molecules/unit cell)	16
mol wt	148.12
calcd density (g cm ⁻³)	1.860
T (K)	150(2)
μ (mm ⁻¹)	0.540
R_1^a	0.0238
wR_2^b	0.0676

^a R_1 is defined as $\sum |F_o| - |F_c| / \sum |F_o|$ for $I > 2\sigma(I)$. ^b wR_2 is defined as $[\sum [w(F_o^2 - F_c^2)^2] / \sum w(F_o^2)^2]^{1/2}$ for $I > 2\sigma(I)$.

theoretically predicted for $ClSO_2N_3$ (Figure S2 of the Supporting Information).

IR and Raman Spectra of $O_2S(N_3)_2$. The IR (gas phase and Ar matrix) and Raman (solid) spectra of $O_2S(N_3)_2$ are shown in Figure 2, and the observed band positions are compared in Table 2 to the calculated spectra.

The gas-phase IR spectrum of $O_2S(N_3)_2$ is very similar to that of $ClSO_2N_3$. The most significant differences are the missing S–Cl stretch in the Raman spectrum of the diazide and the appearance of two bands for the asymmetric N_3 stretches in the Raman (2163 and 2147 cm^{-1}) and the Ar matrix IR (2151.0 and 2135.1 cm^{-1}) spectra. The latter observations unambiguously indicate the presence of two azido groups in the compound.

According to the DFT calculations, two conformers depending on the relative orientation (syn and anti) of the two azido groups with respect to the NSN plane were found to be true minima on the potential energy surface. The two conformers have similar IR spectra (Table 2). However, predicted band intensities and a substantial conformer-shift of the asymmetric and symmetric NSN stretches are features that discriminate between the two conformers. It has been known that IR spectra of matrix isolated species enable the identification of different conformers.²³ As can be seen in Figure 2 (upper trace), two bands appear in the range of 700–800 cm^{-1} in the Ar matrix IR spectrum (Figure 2, upper trace) at 791.2 and 744.1 cm^{-1} , which correspond to the predicted values for $\nu_{as}(NSN)$ and $\nu_s(NSN)$ respectively of the anti conformer (763 and 726 cm^{-1}) rather than those for the syn form (742 and 741 cm^{-1}). Support for this assignment comes from its relative band intensities. In the Raman spectrum, only one strong band at 744 cm^{-1} was observed in this region and it is assigned to the symmetric NSN stretch. The asymmetric one is missing due to their much lower Raman activity. The Ar matrix IR spectra of bis-¹⁵N labeled $O_2S(N_3)_2$ have been measured (Figure S3 of the Supporting Information). In addition to the naturally occurring ³⁴S isotopic splittings, most of the bands are accompanied by satellite bands due to different matrix sites in the solid Ar host (Figure 2, upper trace). The IR

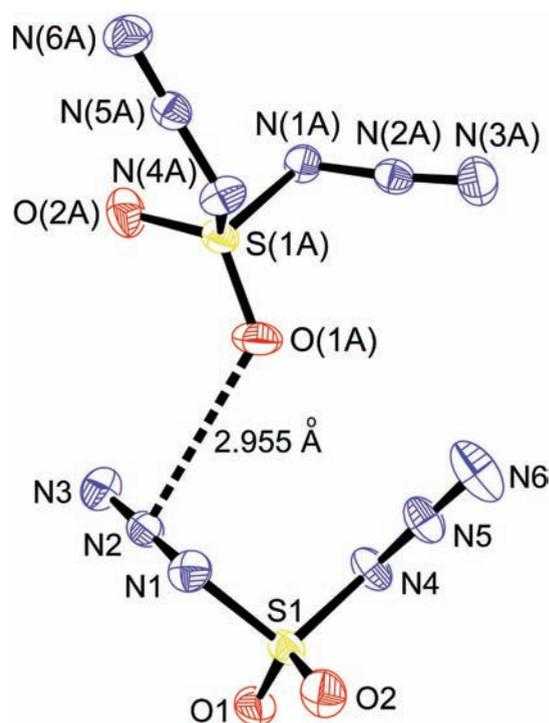


Figure 3. View of the two crystallographically nonequivalent molecules of $O_2S(N_3)_2$; thermal ellipsoids are drawn at the 50% probability level.

and Raman spectra indicate the presence of only the anti conformer in the gas and solid states.

Crystal Structure of $O_2S(N_3)_2$. Sulfuryl diazide crystallizes in the monoclinic space group ($C2/c$) with two crystallographically nonequivalent molecules in the unit cell (Table 3). Weak intermolecular interaction between the two molecules is evidenced by the $N2 \cdots O1$ distance of 2.955 Å, which is shorter than the sum of the van der Waals radii of N (1.55 Å) and O (1.52 Å).²⁴ The molecular structures are depicted in Figure 3, and the determined structural parameters are listed in Table 4.

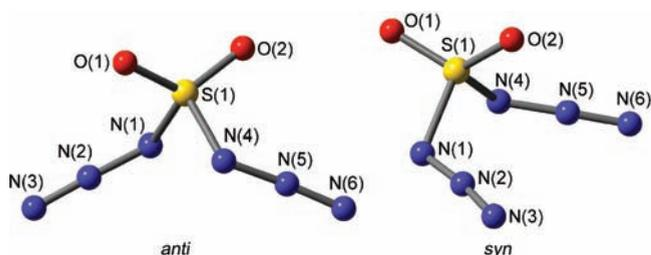
The two azido groups in both molecules are oriented in an anti configuration with respect to the NSN plane, adopting an approximate C_2 symmetry. The S=O bonds (1.4182(9), 1.4180(9), 1.4172(9), and 1.4158(10) Å) are slightly longer than those found in solid FSO_2N_3 (1.411(2) and 1.402(2) Å),⁵ and the S–N bonds in the diazide (1.6709(11), 1.6641(10), 1.6636(10), 1.6654(10) Å) are much longer than that in FSO_2N_3 (1.648(3) Å).⁵ These differences can be attributed to the lower electronegativity of the ligand N_3 relative to F. The OSO angles (122.92(6) and 122.35(6)°) are very similar to that in FSO_2N_3 (122.82(15)°).⁵

Quantum Chemical Calculations. The molecular structures of $ClSO_2N_3$ and $O_2S(N_3)_2$ were fully optimized using different DFT methods (B3LYP, BP86, MPW1PW91) and the 6-311+G(3df) basis set. Similar to other sulfuryl monoazides, only one conformer was predicted for $ClSO_2N_3$ (Figure S2 of the Supporting Information). Two conformers were found for the diazide, which differ by the orientation of the two azido groups (Figure 4). The CBS-QB3 calculations predict the anti (C_2) conformer to be 6.6 $kJ mol^{-1}$ lower in energy than the syn (C_s) one. According to the CBS-QB3 method, the Gibbs free energies of the two conformers are very similar, and the anti one was calculated to be lower by 2.3 $kJ mol^{-1}$ (ΔG , 298 K). From the

Table 4. Calculated and Experimental Structural Parameters of $O_2S(N_3)_2$

parameters ^a	calculated ^b		experimental X-ray crystallography
	anti (C_2)	syn (C_s)	
R(S1–O1)	1.421	1.415	1.4182(9)/1.4180(9)
R(S1–O2)	1.421	1.430	1.4172(9)/1.4158(10)
R(S1–N1)	1.698	1.697	1.6709(11)/1.6641(10)
R(S1–N4)	1.698	1.697	1.6636(10)/1.6654(10)
R(N1–N2)	1.244	1.242	1.2633(16)/1.2648(14)
R(N2–N3)	1.119	1.120	1.1146(15)/1.1094(15)
R(N4–N5)	1.244	1.242	1.2659(14)/1.2630(14)
R(N5–N6)	1.119	1.120	1.1123(16)/1.1103(15)
\angle (O1S1O2)	124.1	124.2	122.92(6)/122.35(6)
\angle (O1S1N1)	109.9	104.7	110.54(6)/102.72(5)
\angle (O2S1N4)	109.9	109.5	111.63(5)/103.63(5)
\angle (N1S1N4)	102.5	102.1	104.84(5)/105.05(5)
\angle (S1N1N2)	115.0	115.6	113.07(8)/112.40(7)
\angle (S1N4N5)	115.0	115.6	112.61(7)/113.13(8)
\angle (N1N2N3)	173.8	173.7	173.09(11)/173.21(12)
\angle (N4N5N6)	173.8	173.7	172.99(12)/172.79(12)
ϕ (O1S1N1N2)	–30.6	–154.6	–33.84(11)/–34.52(11)
ϕ (O2S1N4N5)	–30.6	19.5	–45.70(10)/–44.07(11)

^aBond lengths and angles are given in Å and deg, respectively; for labeling of atoms see Figure 3. ^bAt the B3LYP/6-311+G(3df) level of theory; molecule symmetry is indicated in parentheses.

**Figure 4.** Calculated two conformers of $O_2S(N_3)_2$.

experimental observation of only the anti conformer in the solid and gaseous states, we estimate the difference of ΔG for two conformers should be larger than 6 kJ mol^{-1} .

The preference of the anti conformation may partially be attributed to the steric repulsion between the two azido groups. In addition, anomeric interactions between the α -nitrogen lone pairs and the antibonding orbital of the antiperiplanar $S=O$ bond has been suggested to contribute to the energetic stabilization of the most abundant conformer of the sulfonyl azides (FSO_2N_3 and $CF_3SO_2N_3$).⁵ As a side proof to the existence of the anomeric $n_\sigma(N_\alpha) \rightarrow \sigma^*(S-O)$ interactions, the $S1=O2$ bond in the syn conformer (1.430 Å) was theoretically found to be longer than the two $S=O$ bonds in the anti conformer (1.421 Å), and the shortest one is the $S1=O1$ bond in the syn conformer (1.415 Å). The anomeric interactions should also stabilize anti more than syn due to two favorable $n_\sigma(N1) \rightarrow \sigma^*(S1-O1)$ and $n_\sigma(N4) \rightarrow \sigma^*(S1-O2)$ interactions compared to the two competing nitrogen lone pair interactions to one $\sigma^*(S1-O2)$ in the syn conformer. This is supported by NBO calculations which

predicted a larger $n_\sigma(N_\alpha) \rightarrow \sigma^*(S-O)$ delocalization interaction energy ($E(2)$) for the anti (44.3 kJ mol^{-1}) than that for the syn conformer (38.8 kJ mol^{-1}).

CONCLUSIONS

The previously reported explosive sulfonyl diazide, $O_2S(N_3)_2$, was isolated in pure form and characterized by IR (gas phase and Ar matrix) and Raman (solid) spectroscopy. Its structure was determined by X-ray crystallography. The diazide melts at -15°C and does not decompose at room temperature. It can be transferred at the vacuum line by vaporization at room temperature. Two conformers with similar energy were predicted for $O_2S(N_3)_2$ by the DFT methods, but only the more stable anti conformer was observed in gas and solid phases. The related chlorosulfonyl azide, $ClSO_2N_3$, was also prepared and characterized by IR and Raman spectroscopy.

ASSOCIATED CONTENT

S Supporting Information. UV spectra of $O_2S(N_3)_2$ and $ClSO_2N_3$ in the gas phase, calculated structure of $ClSO_2N_3$ at the B3LYP/6-311+G(3df) level, Ar matrix IR spectrum of bis-¹⁵N labeled $O_2S(N_3)_2$, 3D image of the crystal packing of $O_2S(N_3)_2$, and the X-ray crystallographic file in CIF format of the structure determination of $O_2S(N_3)_2$. This material is available free of charge via the Internet at <http://pubs.acs.org>.

AUTHOR INFORMATION

Corresponding Author

*E-mail: zeng@uni-wuppertal.de.

ACKNOWLEDGMENT

This work was supported by the Deutsche Forschungsgemeinschaft (DFG) and the Fonds der Chemischen Industrie.

REFERENCES

- (1) See recent reviews: (a) Bräse, S.; Gil, C.; Knepper, K.; Zimmermann, V. *Angew. Chem., Int. Ed.* **2005**, *44*, 5188–5240. (b) Knapp, C.; Passmore, J. *Angew. Chem., Int. Ed.* **2004**, *43*, 834–4836. (c) Tornieporth-Oetting, I. C.; Klapötke, T. M. *Angew. Chem., Int. Ed.* **1995**, *34*, 511–520.
- (2) See recent examples: (a) Lyhs, B.; Bläser, D.; Wölper, C.; Schulz, S. *Chem.–Eur. J.* **2011**, *17*, 4914–4920. (b) Schulz, S.; Lyhs, B.; Jansen, G.; Bläser, D.; Wölper, C. *Chem. Commun.* **2011**, *47*, 3401–3403. (c) Schulz, A.; Villinger, A. *Organometallics* **2011**, *30*, 284–289. (d) Portius, P.; Fowler, P. W.; Adams, H.; Todorova, T. Z. *Inorg. Chem.* **2008**, *47*, 12004–12009. (e) Goebel, M.; Karaghiosoff, K.; Klapötke, T. M. *Angew. Chem., Int. Ed.* **2006**, *118*, 6183–6186.
- (3) See recent examples: (a) Klapötke, T. M.; Krumm, B.; Scherr, M. *Inorg. Chem.* **2008**, *47*, 4712–4722. (b) Klapötke, T. M.; Krumm, B.; Scherr, M.; Haiges, R.; Christe, K. O. *Angew. Chem., Int. Ed.* **2007**, *46*, 8686–8690. (c) Klapötke, T. M.; Krumm, B.; Polborn, K. J. *Am. Chem. Soc.* **2004**, *126*, 710–711. (d) Haiges, R.; Boatz, J. A.; Vij, A.; Gerken, M.; Schneider, S.; Schroer, T.; Christe, K. O. *Angew. Chem., Int. Ed.* **2003**, *42*, 5847–5851.
- (4) See recent examples: (a) Christe, K. O.; Haiges, R.; Wilson, W. W.; Boatz, J. A. *Inorg. Chem.* **2010**, *49*, 1245–1251. (b) Wilson, W. W.; Haiges, R.; Boatz, J. A.; Christe, K. O. *Angew. Chem., Int. Ed.* **2007**, *46*, 3023–3027. (c) Vij, A.; Wilson, W. W.; Vij, V.; Tham, F. S.; Sheehy, J. A.; Christe, K. O. *J. Am. Chem. Soc.* **2001**, *123*, 6308–6313.
- (5) Zeng, X. Q.; Gerken, M.; Beckers, H.; Willner, H. J. *Phys. Chem. A* **2010**, *114*, 7624–7630.

- (6) (a) Christe, K. O.; Gerken, M.; Haiges, R.; Schneider, S.; Schroer, T.; Tsyba, I.; Bau, R. *Inorg. Chem.* **2003**, *42*, 416–419. (b) Christe, K. O.; Boatz, J. A.; Gerken, M.; Haiges, R.; Schneider, S.; Schroer, T.; Tham, F. S.; Vij, A.; Vij, V.; Wagner, R. I.; Wilson, W. W. *Inorg. Chem.* **2002**, *41*, 4275–4285.
- (7) Wang, L. J.; Zgierski, M. Z.; Mezey, P. G. *J. Phys. Chem. A* **2003**, *107*, 2080–2084.
- (8) Zeng, X. Q.; Liu, F. Y.; Sun, Q.; Ge, M. F.; Zhang, J. P.; Ai, X. C.; Meng, L. P.; Zheng, S. J.; Wang, D. X. *Inorg. Chem.* **2004**, *43*, 4799–4801.
- (9) Curtius, T.; Schmidt, F. *Ber. Deuts. Chem. Ges.* **1922**, *55B*, 1571–1581.
- (10) (a) Nojima, M. *J. Chem. Soc., Perkin Trans I* **1979**, 1811–1815. (b) Griffiths, J. *J. Chem. Soc. C* **1971**, 3191–3195.
- (11) Zeng, X. Q.; Gerken, M.; Beckers, H.; Willner, H. *Inorg. Chem.* **2010**, *49*, 9694–9699.
- (12) Gombler, W.; Willner, H. *J. Phys. E.: Sci. Instrum.* **1987**, *20*, 1286.
- (13) Schnöckel, H. G.; Willner, H. In *Infrared and Raman Spectroscopy, Methods and Applications*; Schrader, B., Ed.; VCH: Weinheim, 1994.
- (14) Zeng, X. Q.; Gerken, M.; Beckers, H.; Willner, H. *Inorg. Chem.* **2010**, *49*, 3002–3010.
- (15) *CrysAlisPro*, Version 1.171.33.42, Oxford Diffraction Ltd.
- (16) Sheldrick, G. M. *SHELXTL97*; University of Göttingen; 1997.
- (17) Becke, A. D. *J. Chem. Phys.* **1993**, *98*, 5648–5652.
- (18) Perdew, J. P. *Phys. Rev. B* **1986**, *33*, 8822–8824.
- (19) Adamo, C.; Barone, V. *J. Chem. Phys.* **1998**, *108*, 664–675.
- (20) Montgomery, J. A., Jr.; Frisch, M. J.; Ochterski, J. W.; Petersson, G. A. *J. Chem. Phys.* **2000**, *112*, 6532–6542.
- (21) Reed, E.; Curtiss, L. A.; Weinhold, F. *Chem. Rev.* **1988**, *88*, 899–926.
- (22) Frisch, M. J.; Trucks, G. W.; Schlegel, H. B.; Scuseria, G. E.; Robb, M. A.; Cheeseman, J. R.; Montgomery, J. A., Jr.; Vreven, T.; Kudin, K. N.; Burant, J. C.; Millam, J. M.; Iyengar, S. S.; Tomasi, J.; Barone, V.; Mennucci, B.; Cossi, M.; Scalmani, G.; Rega, N.; Petersson, G. A.; Nakatsuji, H.; Hada, M.; Ehara, M.; Toyota, K.; Fukuda, R.; Hasegawa, J.; Ishida, M.; Nakajima, T.; Honda, Y.; Kitao, O.; Nakai, H.; Klene, M.; Li, X.; Knox, J. E.; Hratchian, H. P.; Cross, J. B.; Adamo, C.; Jaramillo, J.; Gomperts, R.; Stratmann, R. E.; Yazyev, O.; Austin, A. J.; Cammi, R.; Pomelli, C.; Ochterski, J. W.; Ayala, P. Y.; Morokuma, K.; Voth, G. A.; Salvador, P.; Dannenberg, J. J.; Zakrzewski, V. G.; Dapprich, S.; Daniels, A. D.; Strain, M. C.; Farkas, O.; Malick, D. K.; Rabuck, A. D.; Raghavachari, K.; Foresman, J. B.; Ortiz, J. V.; Cui, Q.; Baboul, A. G.; Clifford, S.; Cioslowski, J.; Stefanov, B. B.; Liu, G.; Liashenko, A.; Piskorz, P.; Komaromi, I.; Martin, R. L.; Fox, D. J.; Keith, T.; Al-Laham, M. A.; Peng, C. Y.; Nanayakkara, A.; Challacombe, M.; Gill, P. M. W.; Johnson, B.; Chen, W.; Wong, M. W.; Gonzalez, C.; Pople, J. A. *Gaussian 03*, revision D.01; Gaussian, Inc.: Wallingford, CT, 2003.
- (23) Barnes, A. J. In *Matrix Isolation Spectroscopy*; Barnes, A. J.; Orville-Thomas, W. J.; Müller, A.; Gaufrés, R., Eds.; NATO ASI, Series C; Reidel Publishing: Dordrecht, The Netherlands, 1981; Vol. 76.
- (24) Bondi, A. *J. Phys. Chem.* **1964**, *68*, 441–451.